Available online at www.sciencedirect.com

ScienceDirect

Procedia Engineering 10 (2011) 3483–3489

Engineering Procedia

ICM11

Modelling competitive delamination and debonding phenomena in composite T-Joints

A. Baldi*, A. Airoldi, M. Crespi, P. Iavarone, P. Bettini

Aerospace Engineering Department – Politecnico di Milano,
Via La Masa 34, 20156 – Milano, ITALY

Abstract

Experimental studies on the failure mode of composite T-joint specimens, in the presence of adhesive interlaminar layers, are presented. Tests underline the role played by the interaction between delamination and debonding phenomena. Quasi static analyses of the tests are performed by means of explicit FE models. A modelling technique based on a cohesive zone approach is adopted to simulate damage propagation both in the adhesive interface and in the most critical interlaminar layers of laminates. All the numerical results are compared against the experimental evidences in terms of fracture patterns, of load vs. displacement responses and local strain levels.

Keywords: Composite T-Joints; Delamination; Debonding; Damage Tolerace; Explicit Numerical Analysis; Cohesive Elements.

1. Introduction

T-joint configuration represents one of the most important joining schemes, which is commonly adopted in aeronautical and marine fields, to efficiently assemble thick composite laminates in primary structural elements [1-3]. Such type of joint undergoes different failure modes depending on load conditions, lay-up sequences and geometrical shapes of the connected laminates. Accordingly, the prediction of T-joint strength and the evaluation of the load carrying capability of a damaged joint can be two critical issues in composite structural design [4]. Numerical simulations can play an important role in order to assist the design of damage tolerant joints and can reduce the number of experiments that are needed to evaluate the structural response in different load conditions and to define optimal design solutions [3]. In such a context, 3D numerical schemes, based on cohesive elements [5-8], have been already successfully employed to analyse the nucleation and subsequent propagation of damage in the

* Corresponding author. Tel.: +39-02-2399-8641; fax: +39-02-2399-8028.
E-mail address: baldi@aero.polimi.it

 doi:10.1016/j.proeng.2011.04.574

adhesive layers of T-joints [2] as well as in the interlaminar layers of the connected sub-laminates. This paper first presents quasi-static three-points bending tests, which have been performed on two T-joint specimens manufactured by means of the adhesion of thick carbon composite laminates. A modelling technique, based on cohesive zone approaches, has been developed and adopted to represent both composite interlaminar layers and bonded connections. The numerical model, which is solved by means of an explicit integration scheme (*Abaqus Explicit*), permits to detect the competitive development of multiple interlaminar damages both in the adhesive interface and in the most critical inner interlaminar layers of laminates and over-laminates. All numerical results are compared against the experimental evidences in terms of fracture patterns, of load vs. displacement curves and local strain trends.

2. Experimental Tests

A series of three-points bending tests have been performed on T-joint composite laminates, adopting a servo hydraulic testing machine (MTS/858) under displacement control of 1 mm/min, as presented in Fig. 1-(A). The specimens, which are sketched in Fig. 1-(B), consist of two thick pre-cured laminates (lateral and central arm), that are joined, in a second curing process, by means of over-laminates with the interposition of a film of structural adhesive. Composite ribbons support the curved part of the over-laminates. Four strain gauges have been placed on the specimens, as reported in Fig. 1-(B).

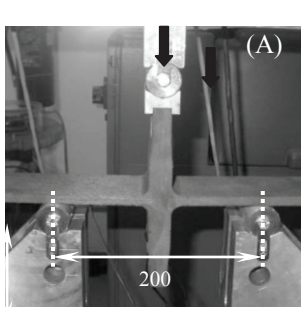

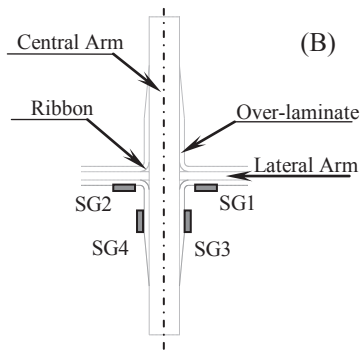

(B)

(C)

	Lateral Arm	Central Arm	Over-laminate
FB $_{@\,45°}$	71.4 %	31.0 %	63.6 %
FB $_{@\,0°}$	28.6 %	58.6 %	36.4 %
UD $_{@\,0°}$	-	10.4 %	-
Thick.	3.92 mm	15.31mm	3.08 mm

Fig. 1. Lay-out of the three-points bending test (A), sketch of the T-joint specimen (B) and ply orientations in the laminates (C)

Specimens have been manufactured by using both a plane wave fabric pre-preg (AS4/8552) and a unidirectional pre-preg (IM7/8552); lay-ups include 0° and ±45° orientations with the percentages reported in Fig. 1-(C). Data relevant to the interlaminar toughness of unidirectional and fabric laminates were obtained in a separate tests campaign, which is described in [9]. The characterisation of the toughness of the adhesive layer is reported in [10]. Fig. 2-(A) presents the force vs. displacement curves of the two T-joint specimens (*TJ-ad-#1* and *TJ-ad-#2*). Although the two specimens exhibit an identical response in the linear phase, the maximum loads reached in the tests are different: 5.2 kN and 4.3 kN for *TJ-ad-#1* and *TJ-ad-#2*, respectively. Such quantitative discrepancy also corresponds to differences detected in the failure modes of the two specimens. Fig. 3-(A) shows the central part of the specimen *TJ-ad-#1* just after the load drop due to the development of an interlaminar damage in the over-laminate. The load decrease from the peak level to a value of about 2.4 kN. Subsequently, the damage has affected the adhesive in the second cure interface between the over-laminate and the central arm, as presented in Fig. 3-(B). Both the cracks in the interlaminar layer and in the adhesive propagated in the downward direction, as shown in Fig. 3-(C).

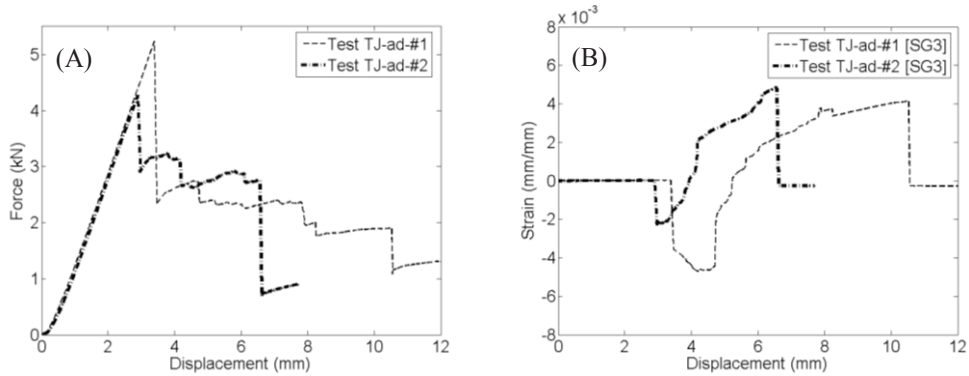

Fig. 2. Load vs. Displacement curve for the T-joint specimens (A) and strain measured by the vertical gage [SG3] (B)

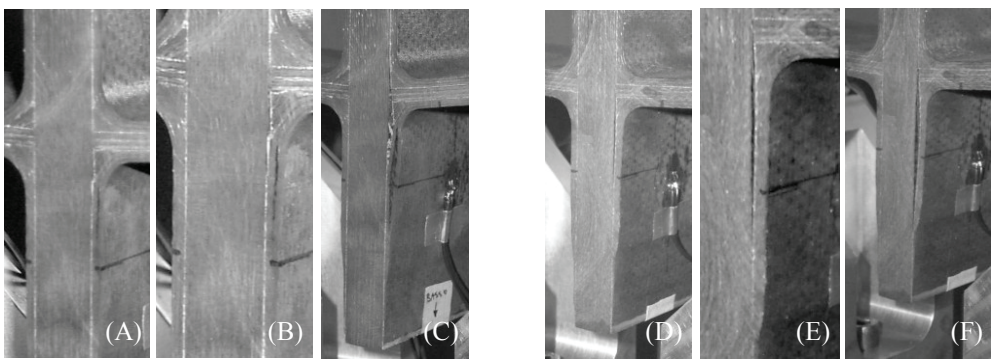

Fig. 3. Evolution of the interlaminar damage for the *TJ-ad-#1* specimen (A)-(B)-(C) and for the *TJ-ad-#2* specimen (D)-(E)-(F)

The failure mode of the *TJ-ad-#2* specimen is characterised by an initial damage that propagates in unstable way that has affected an interlaminar layer of the central arm, as shown in Fig. 3-(D). A close observation of the interface among the central arms, the over-laminates and the ribbons (Fig. 3-(E)) indicates that actually two cracks developed starting from the lower angle of the right-lower triangular ribbon. A first crack originated at one of the interlaminar layer of the central arm and propagated downward, while a second crack propagated upward in the adhesive interface between the central arm and the ribbon. Fig. 3-(F) shows that both the crack developed, but that the final failure has been originated by the complete propagation of the first one, inside the interlaminar phase of the central arm, until the lower end of the specimen. Fig. 2-(B) reports the strain acquired by SG3 during the tests.

3. Numerical approach

An approach based on cohesive zone model is employed to analyze the multiple crack propagation process in the T-joints. The need of modelling potential cracks both in adhesive layer and in the interlaminar layer of composite is pointed out by the experimental evidences. In order to manage a complex model including several interlaminar layers, a numerical approach based on a cohesive zone model has been applied. In the proposed modelling technique, composite laminates are described as a collection of sub-laminates that are represented by bi-dimensional elements, such as membrane or shell elements. The area of each sub-laminate cross section is considered lumped at its mid-plane. The

kinematic variables used to describe the fracture process in mode I, II and III are the relative displacements at the mid-planes of such sub-laminates (Fig. 4-(A)). The components of the relative displacement vector ($\Delta=U^{+}-U^{-}$) can be associated to the three possible modes of fracture openings, as indicated in Eq. 1.

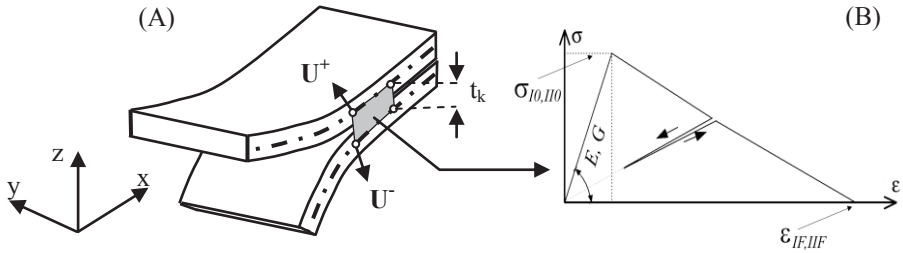

Fig. 4. Description of the interlaminar fracture process in the proposed modeling approach (A) and bi-linear constitutive law (B)

$$\Delta_I = \begin{cases} \Delta_z & if \quad \Delta_z > 0 \\ 0 & if \quad \Delta_z \le 0 \end{cases} \; ; \; \Delta_{II} = \Delta_x \; ; \; \Delta_{III} = \Delta_y \tag{1}$$

Within a small strain assumption, the vector Δ can also be related to the average value of out-of-plane strain components acting in the material volume between the sub-laminates with thickness t_k (Eq. 2).

$$\boldsymbol{\varepsilon} = \left\{ \varepsilon_{zz} \quad \gamma_{xz} \quad \gamma_{yz} \right\}^{T} = \boldsymbol{\Delta} / t_k \tag{2}$$

Conventional solid elements are used to connect the bi-dimensional elements and to represent a generic interface. The response of the connection element can be modelled as in Eq. 3, where a scalar damage variable has been introduced to model the fracture process.

$$\begin{Bmatrix} \sigma_{zz} \\ \tau_{xz} \\ \tau_{yz} \end{Bmatrix} = \begin{bmatrix} E_{zz} & 0 & 0 \\ 0 & G_{xz} & 0 \\ 0 & 0 & G_{yz} \end{bmatrix} (1-d) \begin{Bmatrix} \varepsilon_{zz} \\ \gamma_{xz} \\ \gamma_{yz} \end{Bmatrix} \tag{3}$$

The resulting finite element scheme, made of bi-dimensional elements which represent the composite plies connected by solid elements with null in-plane response, guarantees the translational equilibrium of each sub-laminate included in the laminate lay-up, as presented in [9-11]. The capability of the technique to model the bending response of composite laminates has been assessed by several numerical benchmarks and by the correlations with experimental tests reported in [9-11]. Globally, it should be observed that the proposed approach does not introduce free surfaces that do not exist at the beginning of the computation and does not require the traditional cohesive elements with infinitesimal or zero thickness. As a consequence, all the material characteristics can be directly determined on the basis of physical considerations. The approach can be considered well suitable to model laminates with several interfaces, all of them representing a potential location of damage onset, and to limit the computational costs of analyses carried out by means of explicit finite element scheme.

The onset and the evolution of the damage variable introduced in Eq. 3 can be set to model the strength and the toughness of the interlaminar layers. To accomplish such objective, the proposed approach

exploits the links between the critical energy release rates and the energy dissipated in the damage process [6]. Taking into consideration Eq. 2, the link between the strain-stress response and the energy release rates for fractures opening in mode I and II can be expressed as in Eq. 4. Throughout this work, a bi-linear response has been adopted for the cohesive law, as in [6]. The law is implemented into a stress-strain model thanks to the Eq. 2 and Eq. 4, and attributed to the solid elements. Figure 4-(B) shows the modelled bi-linear response. Properties in mode II and mode III are considered identical. Mixed mode processes are addressed by introducing both strength and toughness criterion, as described by several authors [6, 12]. A quadratic strength criterion has been employed for strength, as in [6], whereas the mixed-mode toughness criterion proposed by Benzeggagh and Kenane has been implemented (B-K criterion). In the criterion, expressed in Eq. 5, the empirical parameter η has been set equal to 1.45 [6]. In such form, the cohesive law has been implemented in a *Fortran Vumat* subroutine to be linked to the *Abaqus Explicit Code*.

$$\int_0^\infty \sigma_{zz} d\Delta_I = t_k \int_0^\infty \sigma_{zz} d\varepsilon_{zz} = G_{Ic} \quad ; \quad \int_0^\infty \tau_{xz} d\Delta_{II} = t_k \int_0^\infty \tau_{xz} d\gamma_{zx} = G_{IIc} \tag{4}$$

$$G_C = G_{IC} + \left(G_{IIC} - G_{IC}\right)\left(\frac{G_{II}}{G_T}\right)^{\eta} \quad \text{, with} \quad G_T = \left(G_I + G_{II}\right) \tag{5}$$

4 Numerical vs. experimental correlation

The proposed numerical approach has been adopted to model the T-joint specimen, as shown in Fig. 5-(A). The over-laminates and lateral arms have been divided into six sub-laminates, which have been modelled by shell elements (S4R [13]) and connected by conventional solid elements (C3D8R [13]), which implement the cohesive zone model. The external layers of the central arm, close to the adhesive interface, have been modelled by means of four sub-laminates. The shell elements have been characterised with the in-plane elastic properties reported in [9, 10], whereas cohesive solid elements have been characterised by the following out-of plane stiffness properties: E_{33} = 7.8 GPa and $G_{13} = G_{23}$ = 5 GPa, for all the interlaminar layer of the model. The interlaminar constitutive model has been completed by means of the fracture toughness and the strength values presented in Table 1. All the interlaminar strength values have been identified by means of experimental-numerical correlations, which also included tests on T-joints carried out without adhesive [9, 10].

Table 1. Interlaminar strength and toughness values of the different interfaces in the T-joint model

Interlaminar Properties	Fabric-Fabric	UD-UD	Fabric-UD	Adhesive
σ_{I0} / σ_{II0} (MPa)	45 / 80	45 / 80	55 / 70	45 / 55
G_{Ic} / G_{IIc} (kJ/m^2)	1.064 / 1.750	0.344 / 0.583	0.704 / 1.167	0.208 / 3.033

A continuum shell scheme has been employed to model the tips of the lateral arms and the inner part of the central arm, in order to reduce the computational cost of the model. Rollers have been modelled by means of rigid cylindrical surfaces. The light alloy tab between the central cylinder and the central arm has been also included in the model. The medium size of the elements on the plane of laminates varies from 2 mm to 2.33 mm, in agreement with the prescription reported in [14] for cohesive zone approaches. Failure has been induced at one side of the model by artificially increasing the interlaminar strengths of 10% at the other side. The numerical model fails at a peak load of 4.8 kN, which it is between the strength values of the two tested specimens, as it is shown in Fig. 6-(A). The comparison between the numerical

and experimental results for the *TJ-ad-#2* specimen underlines the capability of the proposed cohesive approach to capture the competitive development of multiple interlaminar damages within the interlaminar layer of the central arm and in the adhesive interface, as reported in Fig. 5-(B)-(C).

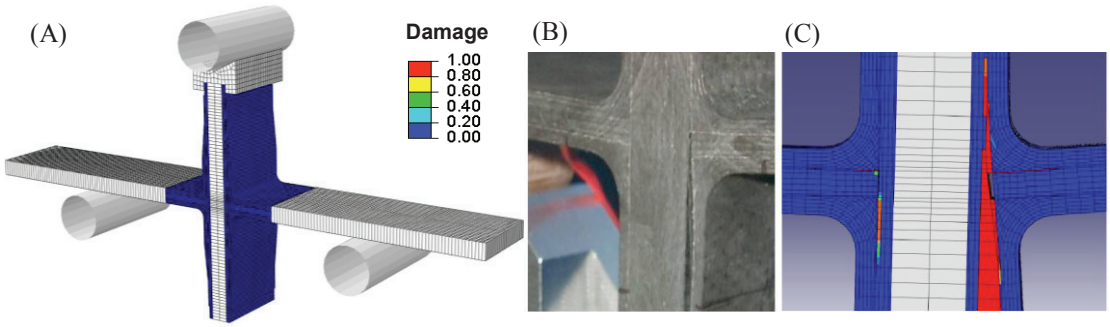

Fig. 5. FE model of the T-joint specimen adopting the proposed cohesive modeling technique (A); experimental evidence of competitive delamination and debonding phenomena in the *TJ-ad-#2* specimen (B) and numerical interlaminar damage (C)

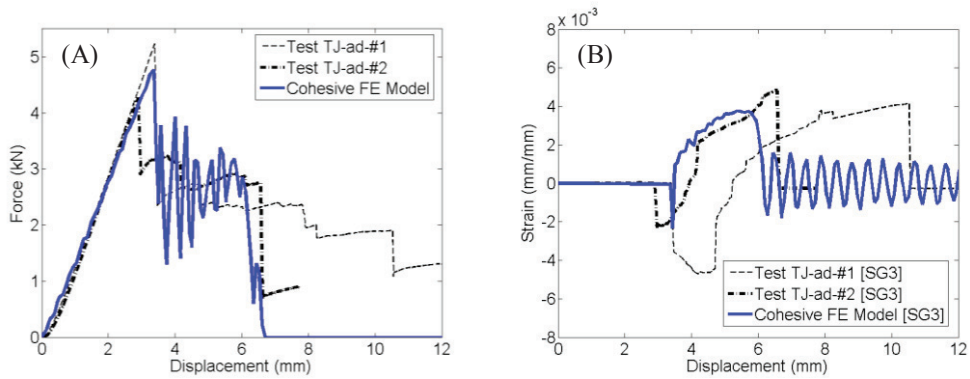

Fig. 6. Numerical-experimental correlation in terms of force vs. displacement response (A) and in terms of strain vs. displacement response (B)

The instable propagation of the interlaminar crack, which is nucleated in the most external interface on the central arm, is correctly identified by the numerical model, as confirmed by the sudden load drop after the peak load level. The stable propagation of the crack, at a plateau load level of about 2.8 kN, is also correctly identified by the numerical model, in good agreement with the experimental evidences. The final detachment of the over-laminate is predicted by the numerical model, at about 6.5 mm of vertical displacement, in good agreement with the results of *TJ-ad-#2* specimen. The numerical strain at the location of SG3 exhibits a very rapid variation from compressive to tensile state. The variation has been also recorded in the experiments, but the numerical progressive increment of positive strain anticipates the experimental course. Such result clearly indicates that the numerical model overestimates the propagation length of the crack during its unstable mode, which immediately follows the load peak. The limitation of the model to correctly identify the debonding of the adhesive interface can be explained by the limit connected to the adoption of the bi-linear response in the cohesive zone approach, in agreement with the considerations reported in [15].

4. Concluding remarks

The flexural behaviour of composite T-joints in the presence of a structural adhesive film between the joined sub-laminates has been experimentally investigated. A numerical approach based on a cohesive zone model has been applied to simulate the onset and subsequent propagation of interlaminar damages both in adhesive and in interlaminar layers. Numerical-experimental correlations in terms of fracture patterns, load vs. displacement curves confirm the capability of the approach, which is based on explicit finite element computations, to identify the potential zones of damage nucleation and to follow the propagation of the cracks during stable and unstable processes. The variations introduced by manufacturing can be considered one of the main reasons for the discrepancies between the two reported experimental responses. Despite such additional complication, delamination and debonding phenomena have been accurately captured for one of the two test cases and the quantitative results are acceptable for both the considered cases. In the light of all these results the proposed numerical approach appears a promising method to assist the design of damage tolerant composite joints.

References

[1] Bish J, Kedward KT. The Analysis and Design of Tee-Joints for Composite Hull. Structures. *Technical Report, NSWCCD-65-TR-1998/11+CR*; 1997.

[2] Zhou DW, Louca LA, Sauders M. Numerical simulation of sandwich T-joints under dynamic loading. *Composite Part B*; 2008; **39**: 973-985.

[3] Di Bella G, Borsellino C, Pollicino E, Ruisi VF. Experimental and numerical study of composite T-joints for marine application. *International Journal of Adhesion & Adhesives*; 2010; **30**: 347-358.

[4] da Silva LFM, Adams RD. The strength of adhesively bonded T-joints. *International Journal of Adhesion & Adhesives*; 2002; **22**: 311–315.

[5] Davila CG, Camanho PP, de Moura MSFS. Progressive analyses of skin/stringer debonding. *Proceedings of the 16th Technical Conference of American Society for Composites*; 2001; Blacksburg, VA.

[6] Davila CG. Mixed mode decohesion elements for analyses of progressive delaminations. *Proceedings of the 42nd AIAA/ASME/ASCII/AHS/ASC Structures, Structural Dynamics, and Material Conference and Exhibit*; 2001; Seattle, WA, USA.

[7] Hu N, Zemba Y, Okabe T, Yan C, Fukunaga H, Elamarkbi AM. A new cohesive model for simulating delamination propagation in composite laminates under transverse loads. *Mechanics of Materials*; 2008; **40**: 920-935.

[8] De Moura MFSF, Campilho RDSG, Gonçalves JPM. Crack equivalent concept applied to the fracture characterization of bonded joints under pure mode I loading. *Composite Science and Technology*; 2008; **68**: 2224-2230.

[9] Airoldi A, Baldi A, Daleffe M, Sala G, Basaglia M. Analyses of delamination in composite laminates in standard tests and low energy impacts. *Proceedings of the 20th AIDAA Congress*, Milano, June 29-July 3, 2009.

[10] Baldi A, Airoldi A, Domenichini P, Crespi M, Sala G. Analysis of progressive failure of composite T-joints. *Proceedings of the 14th European Conference on Composite Materials (ECCM-14)*; Budapest, June 7-10, 2010.

[11] Airoldi A, Sala G, Bettini P. Evaluation of a numerical approach for the development of interlaminar damage in composite laminates. *Composites Science and Technology*; In Press, DOI: 10.1016/j.compscitech.2009.10.011.

[12] Hu N, Zemba Y, Okabe T, Yan C, Fukunaga H, Elamarkbi AM, A new cohesive model for simulating delamination propagation in composite laminates under transverse loads. *Mechanics of Materials*; 2008; **40**: 920-935.

[13] Abaqus®. Theory and User's Manuals. *Hibbit, Karlsson & Sorensen*. Pawtucket, USA, (2004).

[14] Turon A, Davila CG, Camanho PP, Costa J. An engineering solution for mesh size effect in the simulation of delamination using cohesive zone models. *Engineering Fracture Mechanics*; 2007; **74**: 1665-82.

[15] Bettini P, Airoldi A, Sala G, Di Landro L, Ruzzene M, Spadoni A. Composite Chiral Structures for Morphing Airfoils: Numerical Analyses and Development of a Manufacturing Process. *Composite Part B – Eng.*; 2010; **41** (2): 133-147.